Journal of Physics: Conference Series

PAPER • **OPEN ACCESS**

Turbulence Behind 3D Multi-Scale Sparse Grids

To cite this article: Syed M. Usama *et al* 2018 *J. Phys.: Conf. Ser.* **1101** 012048

IOP Conf. Series: Journal of Physics: Conf. Series **1101** (2018) 012048 doi:10.1088/1742-6596/1101/1/012048

Turbulence Behind 3D Multi-Scale Sparse Grids

Syed M. Usama[1], Jackson Tellez-Alvarez[2], Jacek Kopec[3], Kamil Kwiatkowski[3], Jose-Manuel Redondo[2], Nadeem A. Malik[1*]

[1]Department of Mathematics & Statistics, King Fahd University of Petroleum and Minerals, P.O. Box 5046, Dhahran 31261, Saudi Arabia
[2]Department of Physics, Technical University of Catalonia, BarcelonaTech., Barcelona 08034, Spain
[3]Interdisciplinary Centre for Mathematical and Computational Modelling, Faculty of Physics, University of Warsaw ul. Prosta 6900-838, Poland

E-mail: nadeem_malik@cantab.net

Abstract. A fundamentally new idea in grid generated turbulence is the 3D Sparse Grid (3DS) concept [N. A. Malik. Sparse 3D Multi-Scale Grid Turbulence Generator. US Patent No. US 9,599,269 B2 (2017)] which reduces the effective blockage ratio compared to the 2D flat fractal grids, $\sigma_{3DS} \ll \sigma_{2DF}$, and possess a much greater parameter space which could allow further optimization of the turbulence as compared to the 2D fractal (2DF) grids. Here, we report on some theoretical results regarding blockage ratio reduction in a 3-frame 3DS system, and some results from Direct Numerical Simulations comparing the turbulence characteristics generated by 3DS with Regular (RG) and 2DF grids cases.

1. Introduction to 3D Sparse Grids

One of the most important properties of turbulence is its ability to enhance mixing. This has enumerable applications in chemical and industrial contexts and in many natural systems where turbulence is present, such as drag reduction. The control of turbulence is therefore desired. For example, 2D flat (2DF) square fractal grids have been shown to alter the turbulence

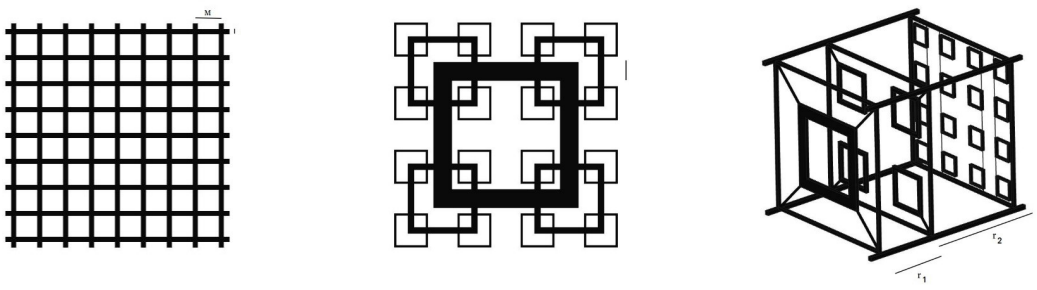

Figure 1: Left to rght: (a) 2D regular grid (RG). (b) 2D fractal square grid (2DF). (c) 3D sparse grid (3DS).

characteristics compared to the regular grids, it is believed that the turbulence intensity is enhanced for the same blockage ratio.

Grid generated turbulence is the most common way of studying turbulence in laboratory experiments. Until recently regular grids (RG), Figure 1(a), with bars of constant thickness producing open cells of constant width for flow passage, have been used. As fractals became popular in the 1990s a new type of grid with bars of different thicknesses and different lengths in a flat 2D fractal arrangement (2DF) was developed, Figure 1(b). The essential idea here is that different scales of turbulence are generated spontaneously in the same plane. The turbulence generated has different characteristics compared to the RGs, with the turbulence intensity peaking at a higher level [1].

A recent innovation in grid generated turbulence, the 3D Sparse Grid (3DS) [2, 3], called the Sparse 3D Multi-Scale Grid Turbulence Generator, or 3D sparse grid (3DS) for short, has excited interest in the turbulence community because of its potential to alter turbulence characteristics downstream of the grid. The 3DS goes further than the 2DF construction by separating each generation of length scale of turbulence grid elements in to its own frame in

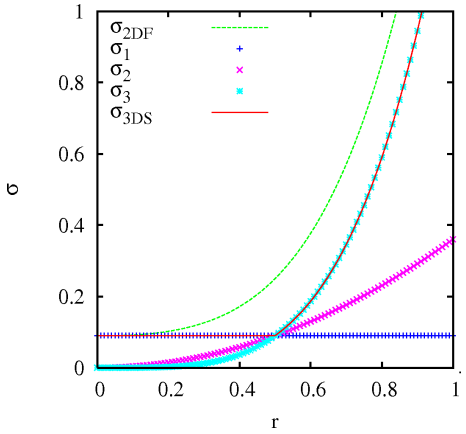

Figure 2: $a = 0.5$, $w_1 = 0.05$

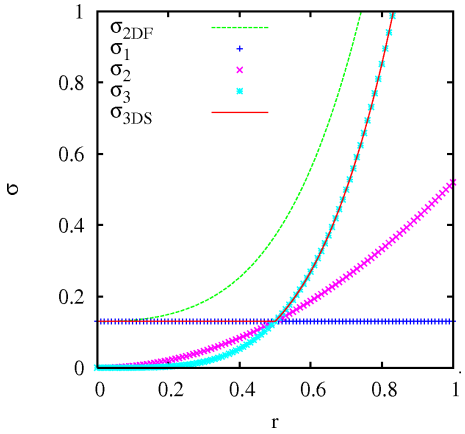

Figure 3: $a = 0.7$, $w_1 = 0.05$

Solidity (blockage ratios) against the scaling factor r. σ_{2DF}, and σ_{3DS}, and the scale-by-scale, $\sigma_1, \sigma_2, \sigma_3$ in the 3DS are shown.

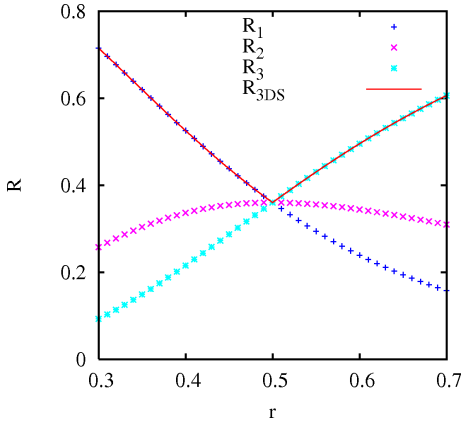

Figure 4: $a = 0.5$, $w_1 = 0.05$

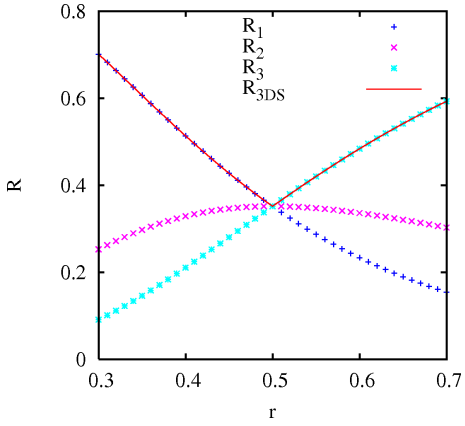

Figure 5: $a = 0.7$, $w_1 = 0.05$

Reduced solidity against the scaling factor r. The scale-by-scale, R_1, R_2, R_3, and R_{3DS} in the 3DSGT are shown.

overall co-planar arrangement, Figure 1(c), which produces a 3D sparse grid system. Each generation of grid elements produces a turbulent wake pattern that interacts with the other wake patterns downstream. The length scale of the grid elements from frame to frame can be in any multiscale ratios, although a fractal pattern is a popular choice.

Here, we report on some theoretical results regarding mass flow rates in 3DS in Section 2, and some results from Direct Numerical Simulations (DNS) that demonstrate the performance of the 3DS in a conduit compared to the classical flat 2D Fractal Grid (2DF) arrangement.

2. Some Properties of 3D Sparse Grids

A direct consequence of separating scales in the 3DS is that the effective blockage ratio (solidity), is greatly reduced compared to the 2DF. Furthermore, the parameter space is increased because the distances between successive frames are additional parameters.

In the 3DS arrangement, the optimal reduction in the blockage ratio as compared to the 2DF flat fractal grid, $R_{3DS}(r) = \sigma_{3DS}(r)/\sigma_{2DF}$, occurs when the geometric ratio between successive length scales is, $r = 0.5$, see Figures 4 and 5. The mass flow rate is increased for the same pressure gradient due to the lower blockage.

Consider a 3-generation 2DF, and a corresponding 3DS sparse arrangement. In both cases, the grids are contained inside a square conduit of height and width equal to H, to give a cross-sectional area of,

$$T \quad = \quad H \times H \tag{1}$$

Suppose that in the first generation (largest scale) the fractal square grid has length $L_1 = aH$, with $a < 1$. The thickness of the grid bars is W_1. The second generation of grid scales is produced from the first generation by scaling with scaling factor r with $0 < r < 1$; thus $L_2 = rL_1$, and $W_1 = rW_0$. In the third generation, $L_3 = r^2 L_1$ and $W_3 = r^2 W_1$.

Then, the 2DF flat grid in Fig. 1, has the total cross-sectional area,

$$A_{2DF} \quad = \quad (L_1 W_1 - W_1^2)(4 + 16r^2 + 64r^4) - W_1^2(8r + 32r^3) \tag{2}$$

This is an exact expression, taking in to account the small overlap areas between the different generations. Laziet & Vassilicos [1] derive an approximate expression in terms of the perimeter

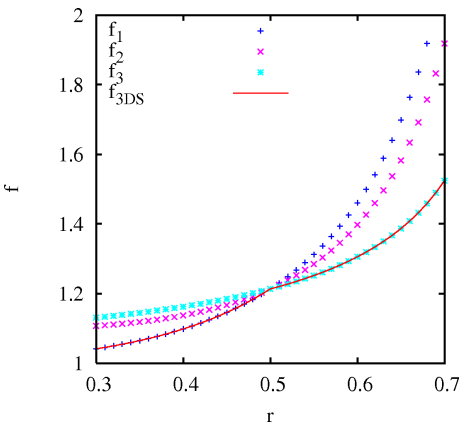

Figure 6: $a = 0.5$, $w_1 = 0.05$

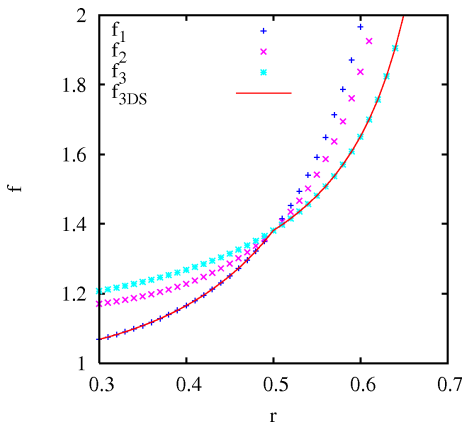

Figure 7: $a = 0.7$, $w_1 = 0.05$

Enhanced mass flux against the scaling factor r. The scale-by-scale, f_1, f_2, f_3, and f_{3DS} in the 3DSGT are shown.

of the square fractal arrangement. The cross-sectional areas for each generation of grid bars in the 3DS separately, are

$$A_1 = 4(L_1W_1 - W_1^2) \quad (3)$$
$$A_2 = 16r^2(L_1W_1 - W_1^2) = 4r^2A_1 \quad (4)$$
$$A_3 = 64r^2(L_1W_1 - W_1^2) = 4r^2A_2 = 16r^4A_1 \quad (5)$$

We non-dimensionalise all lengths by H to obtain the non-dimensional parameters, $l_1 = L_1/H$, and $w_1 = W_1/H$. Then, the blockage ratio (solidity) in the 2D flat grid is given by $\sigma_{2DF} = A_{2DF}/T$,

$$\sigma_{2DF} = (aw_1 - w_1^2)(4 + 16r^2 + 64r^4) - w_1^2(8r + 32r^3) \quad (6)$$

and the solidity of each of grid frame separately in the 3DS are,

$$\sigma_1 = 4(aw_1 - w_1^2);\ \sigma_2 = 4r^2\sigma_1;\ \sigma_3 = 16r^4\sigma_1 \quad (7)$$

The effective solidity of the 3DS arrangement is therefore smaller than the corresponding 2DF,

$$\sigma_{3DS} = Max(\sigma_1, \sigma_2, \sigma_3) \quad (8)$$

The solidity is a function of three non-dimensional variables,

$$\sigma_{3DS} = \sigma_{3DS}(w_1, a, r) < \sigma_{2DF} \quad (9)$$

Figures 2 and 3 show the $\sigma's$ against r for $w_1 = 0.05$, and for $a = 0.5$ and 0.7 respectively.

From equations (7)-(9), for $r = 0.5$ we have $\sigma_1 = \sigma_2 = \sigma_3$. This is because the increase in the number of self-similar squares competes with the decrease in the per unit area from generation to generation. At $r = 0.5$ these two effects exactly balance and lead to the optimal reduction at $r = 0.5$.

We define the reduction in solidity (blockage ratio) from 2DF to 3DS to be,

$$R_\sigma(w_1, a, r) = \frac{\sigma_{3DS}}{\sigma_{2DF}}. \quad (10)$$

We also define scale-by-scale solidity reduction by,

$$R_1 = \frac{\sigma_1}{\sigma_{2DF}};\ R_2 = \frac{\sigma_2}{\sigma_{2DF}};\ R_3 = \frac{\sigma_3}{\sigma_{2DF}}. \quad (11)$$

Figures 4 and 5 shows the solidity reductions R as a function of r, for $w_1 = 0.05$, and for $a = 0.5$ and 0.7 respectively. R_σ shows a minimum of $R_\sigma \approx 0.36$ at $r = 0.5$.

If we approximation the mass flux rate through a grid with blockage ratio σ to be,

$$M = (1 - \sigma)F(Re; \rho, U, \mu, L) \quad (12)$$

where F is some function (for example, F could be proportional to the pressure gradient). ρ is the fluid density, U is the mean flow velocity, ν is the kinematic viscosity Re is the Reynolds number. The increase in mass flow rate from the 2DF flat to the 3DS sparse grids is,

$$f_\sigma(w_1, a, r) = \frac{M}{M_{2DF}} = \frac{1 - \sigma}{1 - \sigma_{2DF}} \quad (13)$$

and similar expressions f_1, f_2, f_3 for each generation can be obtained.

Figures 6 and 7 shows the enhanced mass flow rates, $f's$, against r for the same cases as in Figures 4 and 5 respectively. We obtain $f_\sigma = 1.21$ which is an increase of 21%. Although f_σ continues to increase for $r > 0.5$, the solidity approaches 1, and $1 - \sigma \to 0$, and the flow rate approaches zero. Thus $r = 0.5$ is the optimal enhancement in mass flux rates.

3. Direct Numerical Simulations

The aim here is to compare the turbulence characteristics produced by RG, 2DF, and 3DS grids. We use DNS for this purpose.

The domain is a cuboid of dimensions $460.8 \times 115.2 \times 115.2 d_{min}^3$ where d_{min} is the thickness of the smallest square. Thus, the height and width of the channel is $H = 115.2 d_{min}$. We consider three different grids, regular grid RG, 2D flat fractal grid 2DF, and 3D sparse grid 3DS. The blockage ratios in the RG and 2DF is equal to 32%, and the constant effective mesh size in the RG is $M_{ef} = 13.33 d_{min}$. The bars have length $115.2 d_{min}$ in the RG with thickness $2.6 d_{min}$, the same as in [1].

The bars in the 3DS have the same lengths and thicknesses as in the 2DF. All lengths are henceforth non-dimensionalized by d_{min}.

The 2DF has non-dimensionlized lengths and widths $\{l_i, d_i\}$, in generation $i = 0, 1, 2,$. The geometric ratio for the large grid scales is, $r = 0.5$, and $a = 0.5$. Thus, $l_0 = 57.6 = 0.5h$, $l_1 = 0.5 l_0$, $l_2 = 0.5 l_1$. The geometric ratio for the bar thicknesses is $1/\sqrt{8.5} = 0.34$, thus $d_0 = 8.5$, $d_1 = 2.9 d_2$, $d_2 = 1$.

The time scale is defined by $t_2 = d_{min}/U_\infty$ where U_∞ is the inlet velocity set equal to 1.

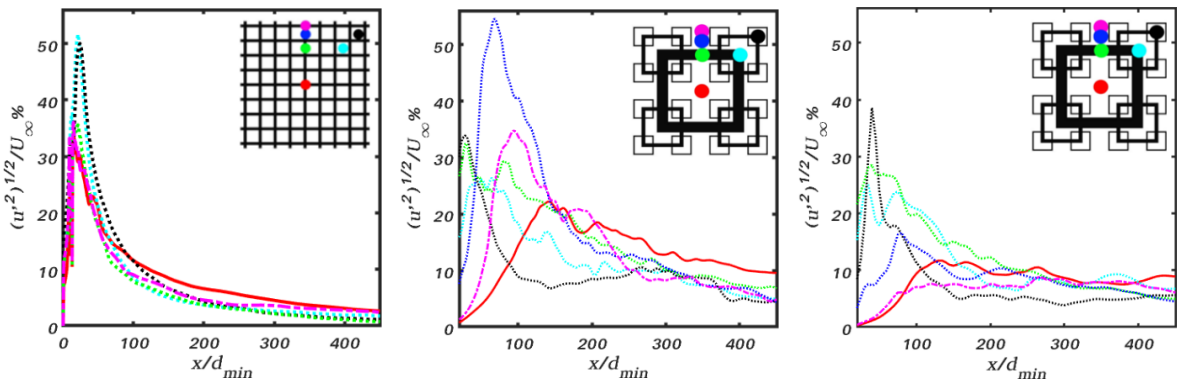

Figure 8: Turbulence intensity along pencils in the channel x-directions. Left: RG; Centre: 2DF; Right: 3DS.

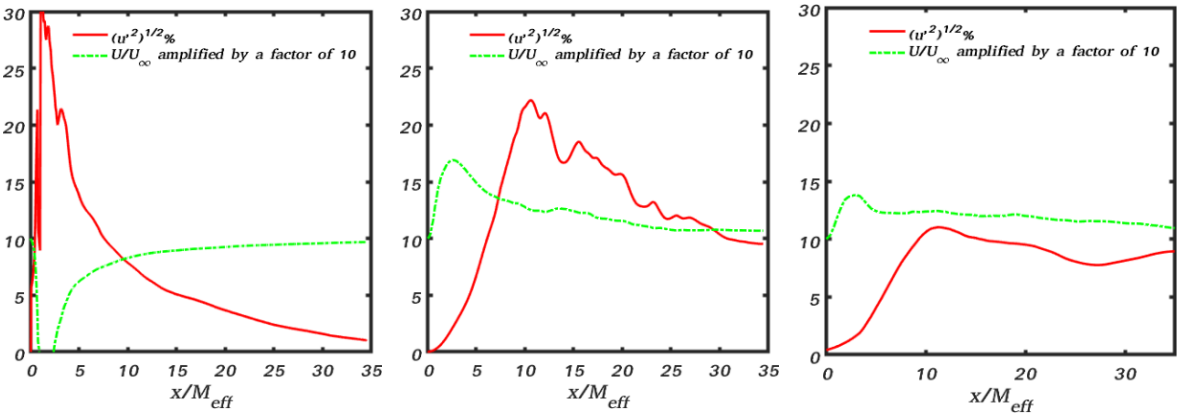

Figure 9: Turbulence intensity along pencils in the channel x-directions. Left: RG; Centre: 2DF; Right: 3DS.

The 3DS has the same lengths and thickness as the 2DF in [1], however each generation is held in a frame separated from the next by non-dimensional distances, $r_1 = x_1 - x_0 = 17$, and $r_2 = x_2 - x_1 = 8.5$, and $x_0 = 10$, where $x_i's$ are the non-dimensionalised x-coordinates of the ith frame.

The solidity (blockage ratio) in the 2DF is 32%, and the solidity in the 3DS is 15%.

To resolve down to the smallest scales, a numerical grid size of one fifth of the thickness of the smallest bar is created, $\Delta x = 0.2 d_{min}$. This creates a grid of $N_x \times N_y \times N_z = 2304 \times 576 \times 576$. The RG and 2DF turbulence grids lie in the plane $x_0 = 10$ downstream of the channel inlet. Periodic boundary conditions are applied on the walls in the y and z directions; and inlet-outlet boundary conditions were applied in the x-direction. The initial condition is a uniform inflow velocity $U_\infty = 1$. The Reynolds number is, $Re = \frac{U_\infty d_{min}}{\nu} = 300$.

OpenFOAM, (OFoam), an opensource CFD toolbox, is chosen for the simulation. OFoam uses finite volume discretization is performed using Pressure Implicit Splitting of Operator Algorithm (PISO). Time discretization using Backward Euler method, whereas gradient and Laplacian term discretization using Gauss linear method are performed. Divergence term discretization is done using Gauss cubic method which is a third order scheme. Interpolation and other terms are discretized using Gauss Linear schemes. The resulting linear systems are solved by preconditioned conjugate gradient method with diagonal incomplete Cholesky preconditioner for pressure solution whereas iterative solver is used with symmetric Gauss-Siedel as the smoother to calculate velocities. Tolerance is set at 10^{-6}. Simulation time step is $\Delta t = 0.015 d_{min}/U_\infty$ which corresponds to a Courant number of 0.75. Probes and pencils are placed at various locations and 100 complete field snapshots have also been recorded in the time range from $300t_2$ to $600t_2$. The flow statistics have also been averaged over this time.

Figures 8-10 shows comparison of turbulence characteristics from RG, 2DF, and 3DS grids from the current DNS simulations. The RG and 2DF plots are close to the results of Laziet & Vassilicos [1], which validates the current DNS for these calculations.

Figure 8 compares the turbulence intensities u'/U_∞ along the channel length in the x-directions – pencils taken at various (y, z) locations as indicated by the different colors. The peak intensities in the 3DS is lower than in 2DF. After about $x/d_{min} = 100$ the intensities in the 3DS is higher and sustained for longer than from the RG, but lower than in 2DF. The latter is probably due to the lower blockage in the 3DS (15%) compared to the 2DF (32%).

Figure 9 shows the plots of the turbulence intensity and the mean flow along the central pencil $(y, z) = (0, 0)$. The mean flows in the 2DF and 3DS are close, and both are significantly

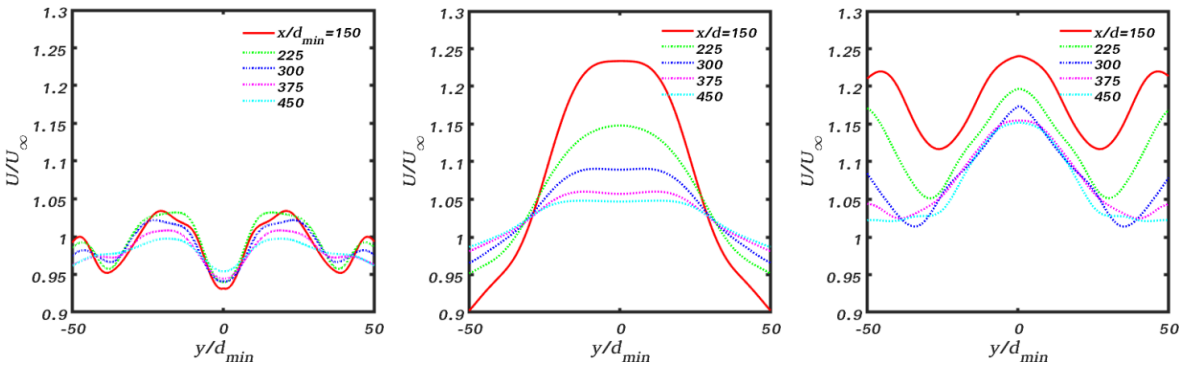

Figure 10: Turbulence intensity along pencils in the channel x-directions. Left: RG; Centre: 2DF; Right: 3DS.

higher than in the RG grid.

Figure 10 shows the mean x-velocity along the y-axis, $U(y)/U_\infty$, taken at different stations along the channel. There is significant difference between the 2DF and 3DS grids. The 2DF grid produces smooth non-oscillating profiles that peak and are uniform in the central region and eventually flatten out further downstream. The results from the 3DS is similar to that from the RG in so far as it shows an oscillating profile across the y-direction, however it shows peak levels similar to the 2DF of about 1.25, compared to the RG where the average is about 1 at all stations along the channel. The 3DS does not flatten out as fast as the 2DF being sustained on average at a higher level further downstream.

The overall impression from the results from the 3DS, with the given configuration, is that the 3DS is roughly in between the RG and 2DF cases for the turbulence characteristics shown.

However, it is important to remember that the blockage ratio in the 3DS is about half of the RG and 2DF so that the mass flow rate in the 3DS turbulence here is about half of that in the other two; to obtain the same flow rate in the RG and 2DF the pressure gradient would have to be doubled, so the mixing efficiency in the 3DS may yet to be greater.

These are the first results from DNS that we have obtained. The aim of this work is a parametric study of 3DS for different r_1 and r_2, and for different blockage ratios, and to address to question of mixing efficiency.

4. Conclusions

The 3DS [2, 3] has been investigated, and some comparisons with the Regular RG and flat 2D fractal grid 2DF has been made. Theoretically, the 3DS admits a higher mass flow rate for the same pressure gradient because of the lower blockage ration (solidity), equation (13). An optimal value for the geometric ratio was found to be 0.5.

DNS was first validated against the previous work of Laziet & Vassilicos [1]. The DNS was then used to simulate RG, 2DF, and 3DS with frame separations of $r_1 = 17d_{min}$ and $r_2 = 8.5d_{min}$ and a blockage ratio of 15%, compared to 32% for the RG and 2DF. It was found that overall the turbulence characteristics generated by 3DS was generally in between the RG and 2DF grids cases; the peak turbulence intensities were lower than in 2DF, and downstream the intensities were also lower than in 2DF. But the intensities were higher than in RG and were sustained for longer downstream.

A critical question is what happens if the blockage ratio of the 3DS is increased towards the 2DF value of 32%. Another is, does 3DS lead to greater mixing efficiency? These issues are currently under investigation numerically. In addition to the velocity field, we are looking at the vorticity field, the pressure field, and diffusing scalar fields.

Acknowledgements

This work has been carried out partly in the framework of European High-Performance Infrastructures in Turbulence (EuHIT) project Trans National Access program at the EuHIT grant, Turbulence Generated by Sparse 3D Multi-Scale Grid (M3SG), 2017.

References

[1] S. Laizet & J. C. Vassilicos. DNS of Fractal-Generated Turbulence. Flow Turbulence Combust 87:673-705 (2011).
[2] N. A. Malik. Sparse 3D Multi-Scale Grid Turbulence Generator. US Patent No. US 9,599,269 B2 (2017).
[3] N. A. Malik. Sparse 3D Multi-Scale Grid Turbulence Generator. EPO Patent no. 2965805 (2017).